LA-UR-03-3458

Title:

Monte Carlo Model for Proton Elastic Scattering from Optical Model Calculations

Author(s):

R. E. Prael, LANL X-5
Lon-Chang Liu, LANL T-16
Sergei Striganov, FNAL

Submitted to:

American Nuclear Society Summer Meeting, June1-5, San Diego (Topical Meeting on Accelerator Applications)

Monte Carlo Model for Proton Elastic Scattering from Optical Model Calculations

R. E. Prael and Lon-Chang Liu
Los Alamos National Laboratory
Sergei Striganov
Fermi National Accelerator Laboratory

Introduction

- A Monte Carlo elastic scattering method was developed for application to proton radiography[1] at high energies.
- The method uses a processed data library derived from optical model calculations for 22 nuclei from A =2 to A = 242 and 47 lab momenta over the range 1 GeV/c to 50 GeV/c.
- With the Monte Carlo sampling method developed for use in MCNP Version 5, the method accurately reproduces the original optical model calculations over a range of 10^7 in cross section and provides good interpolation properties over intermediate masses and energies.

Optical Model Calculations (1)

- The proton-nucleus elastic differential cross sections were calculated for momentum transfers up to 0.85 GeV/c at incident proton laboratory momenta 1 to 50 GeV/c in the framework of eikonal theory.
- In this theory, the proton-nucleus phase shifts at a given impact parameter are obtained from integrating the optical potential along a line perpendicular to that impact parameter[2].
- The matter density was derived from the experimental nuclear charge density by removing the proton charge distribution according to a translationally invariant method[3].

Optical Model Calculations (2)

- Without any free parameter, the calculated differential cross sections describe well the existing data, indicating that effects of higher-order optical potential can be expected to be small.
- In order to examine the applicability of eikonal theory in light nuclear systems, the p-^{3}H and p-^{6}Li elastic differential cross sections given by the eikonal theory were compared with those given by the Glauber theory[6].
- For all the energies and momentum transfers considered, the differences are less than 5% for p-t scattering and become negligible for p-^{6}Li scattering

Optical Model Calculations (3)

- The target masses at present are: ^{2}H, ^{3}H, ^{9}Be, ^{12}C, ^{14}N, ^{16}O, ^{19}F, ^{27}Al, ^{35}Cl, ^{37}Cl, ^{52}Cr, ^{56}Fe, ^{58}Ni, ^{60}Ni, ^{93}Nb, ^{133}Cs, ^{184}W, ^{208}Pb, ^{235}U, ^{238}U, ^{239}Pu, ^{242}Pu
- Examples of the calculated differential cross sections are shown in figure 1.
- In this initial effort, the contribution from nuclear-Coulomb interference has been neglected.
- Proton and neutron densities are each treated as proportional to the nuclear matter densities.

Figure 1

Calculated differential cross section for p+C12

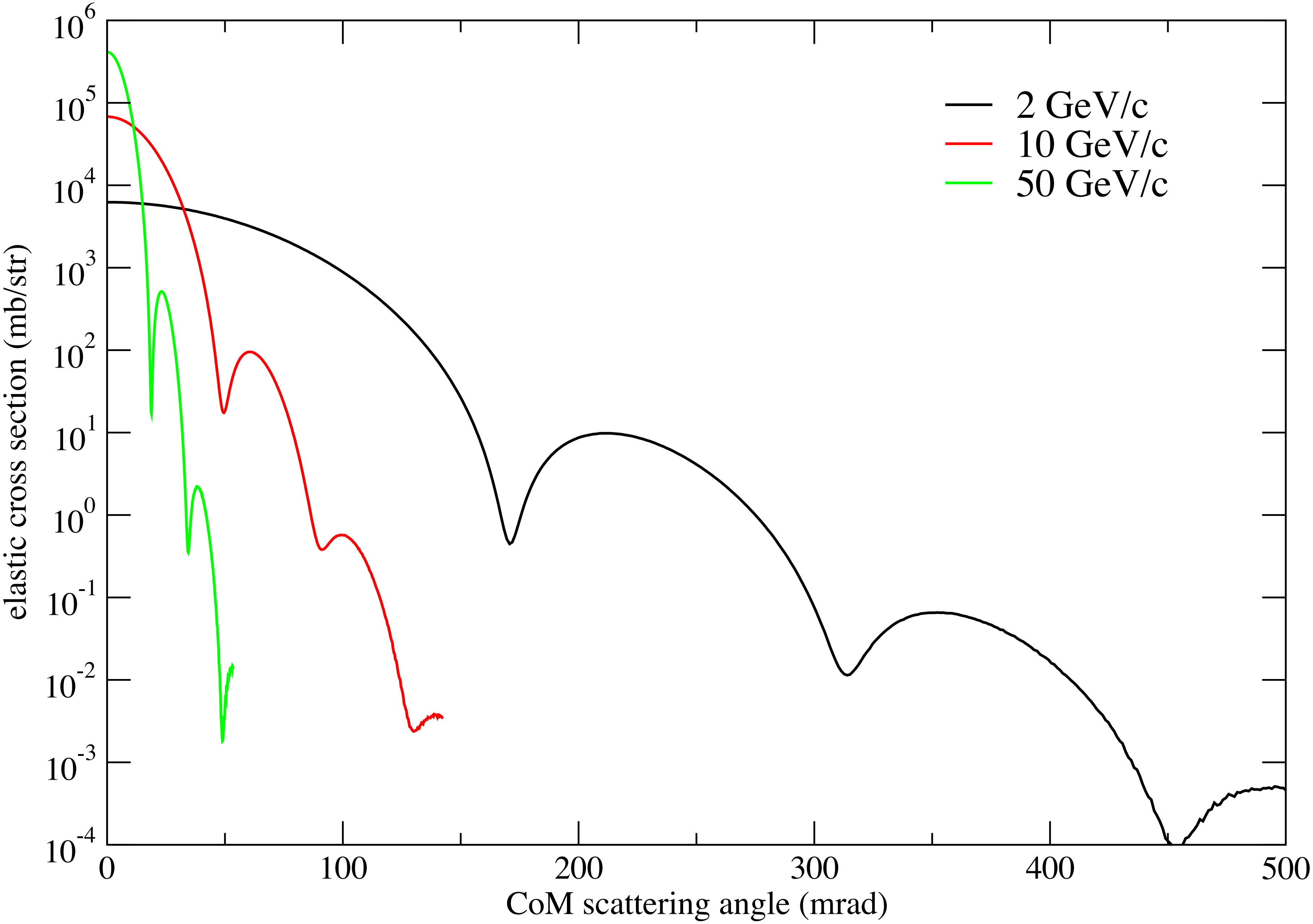

Optical Model Calculations (4)

- In addition, the effects of nuclear deformation are addressed only approximately.
- Effects of the deformation are contained in the measured observables used in the optical model parameters.
- Subsequent treatment as a spherical nucleus provides a “zeroth” order approximation to a full coupled channel calculation of the elastic scattering.
- As a consequence, interpolation on mass is a less reliable approximation in the range 133 < A < 208.

Data Representation (1)

For each mass and energy in the data library, the original cross section calculations are represented as a sampling distribution ***S(X)*** for the dimensionless variable ***X*** where

$$X = q / q_1 = 2p \sin\left(\theta / 2\right) / q_1$$

for center-of-mass momentum ***p***, momentum transfer ***q*** and scattering angle θ.

$$0 \le X \le 2p / q_1$$

Data Representation (2)

The differential cross section is transformed to ***S(X).***

$$f_0(\mu) = \frac{2\pi}{\sigma_{el}} \frac{d\sigma}{d\Omega} \quad \text{for} \quad \mu = \cos(\theta)$$

$$f(X) = f_0(\mu)\left|d\mu / dX\right| = \left(\frac{q_1}{p}\right)^2 X f_0(\mu(X))$$

$$S(X) = \frac{f(X)}{\max\{f(X)\}}$$

Data Representation (3)

- ***S(X)*** is tabulated in the data library along with an "envelope function" ***R(X)*** for each isotope in the library.
- ***R(X)* > *S(X)*** for all the energy dependent distributions of that isotope.
- An example of the functions ***S(X)*** and ***R(X)*** for ^{12}C is shown in figure 2 and for ^{242}Pu in figure 3.
- The representation of ***S(X)*** for 5 isotopes at incident momentum 24 GeV/c is shown in figure 4.

Figure 2

S(X) at 4 energies and R(X) for C12

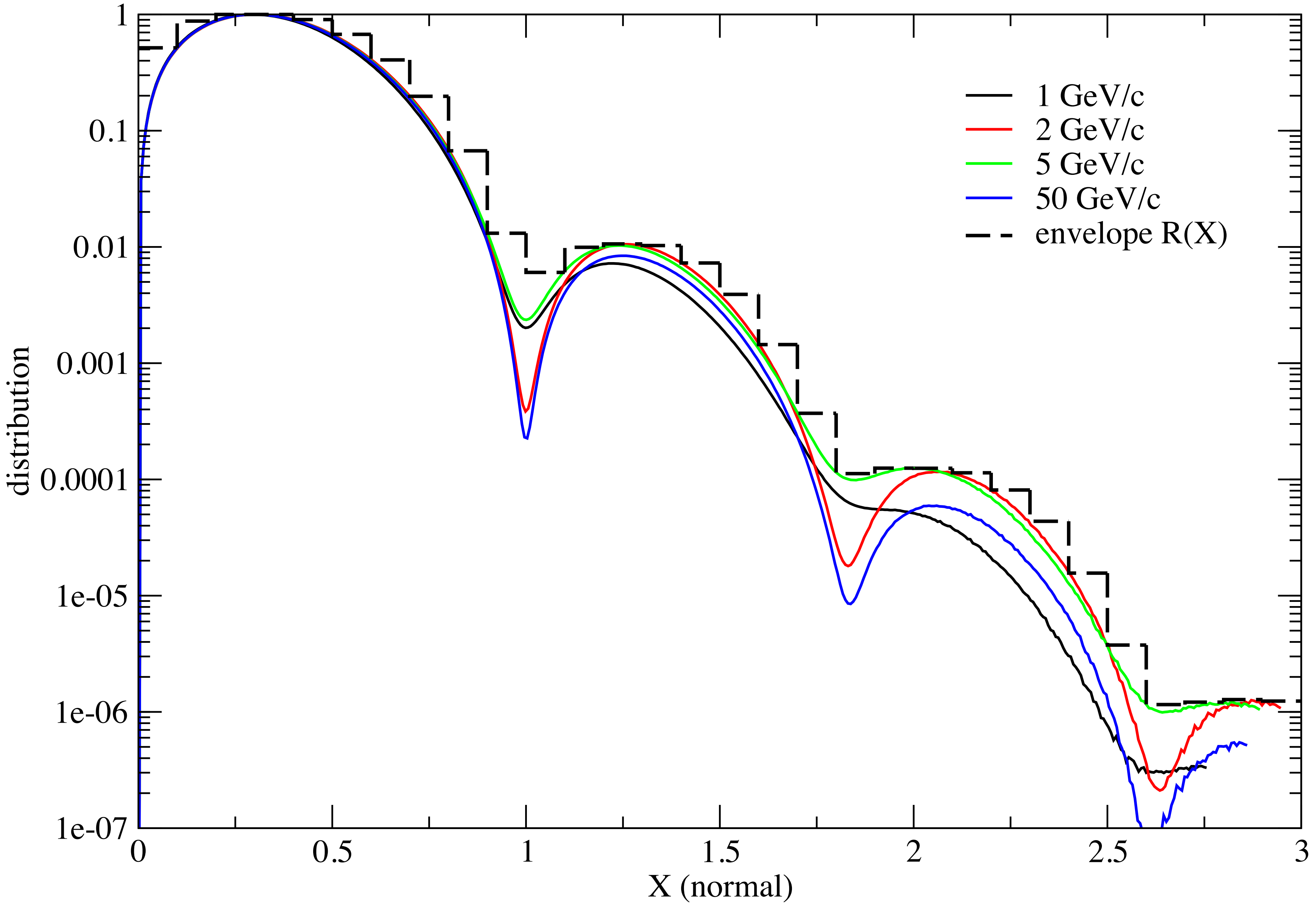

Figure 3

S(X) at 4 energies and R(X) for Pu242

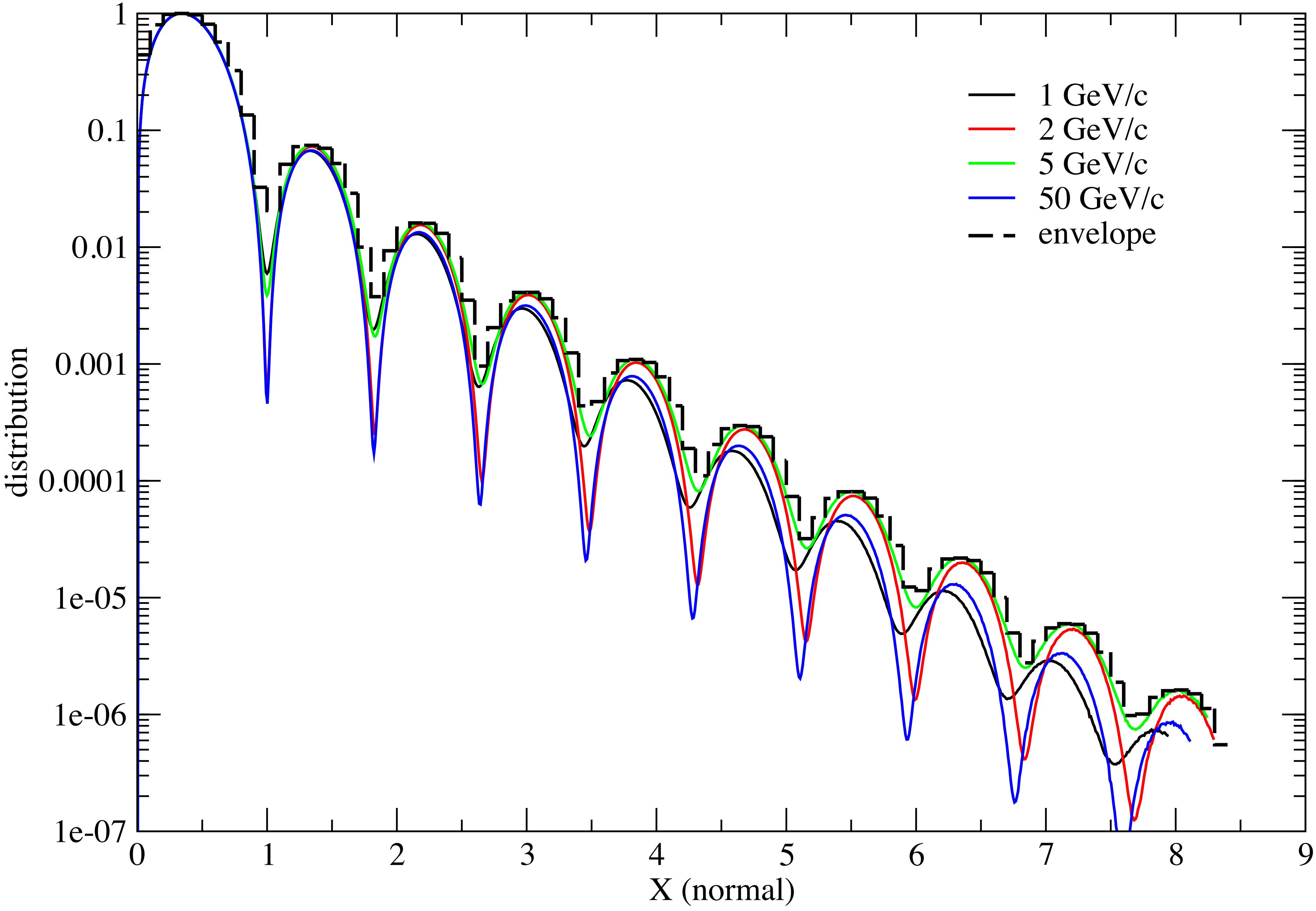

Figure 4

The tabulated function S(X) for 5 isotopes at 24 GeV/c

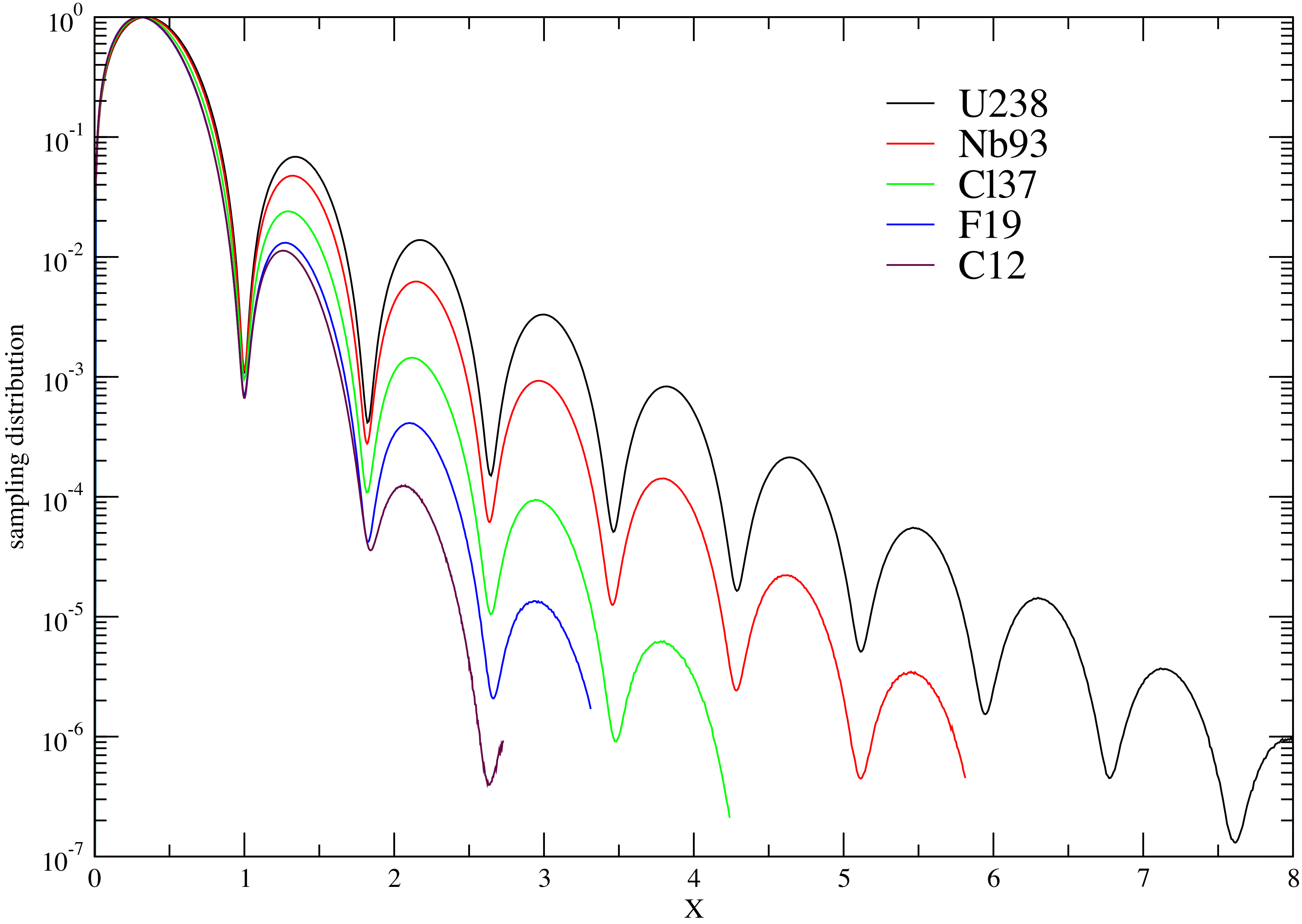

Monte Carlo Algorithm (1)

- Select a single table energy by random linear interpolation on incident particle energy.
- For $A_1 < A < A_2$ or $A = A_2$, sample trial $\boldsymbol{X}$ from histogram distribution $\boldsymbol{R(X)}$ for tabulated mass A_2 .
- Use log-log interpolation to obtain $\boldsymbol{S(X)}$ from tabulations for A_1 and A_2 (if between tabulated isotopes.)
- Use $\boldsymbol{S(X)}$ for rejection sampling to obtain final value of $\boldsymbol{X}$.
- Use inverse equation to obtain $\theta = \theta(X)$ for the center of mass scattering angle.

Monte Carlo Algorithm (2)

- The variable q_1, the momentum transfer at the first diffraction minimum, is tabulated for the same masses and energies.
- $1/q_1$ is proportional to an "effective nuclear radius"; $1/q_1$ varies slowly in energy and roughly as $A^{1/3}$ as shown in figures 5 and 6.
- For any target and energy, the interpolated value of q_1 is used with a sampled value of X to obtain the center of mass scattering angle by inversion of the previous equation.

Figure 5

Variation of q1 with incident particle momentum

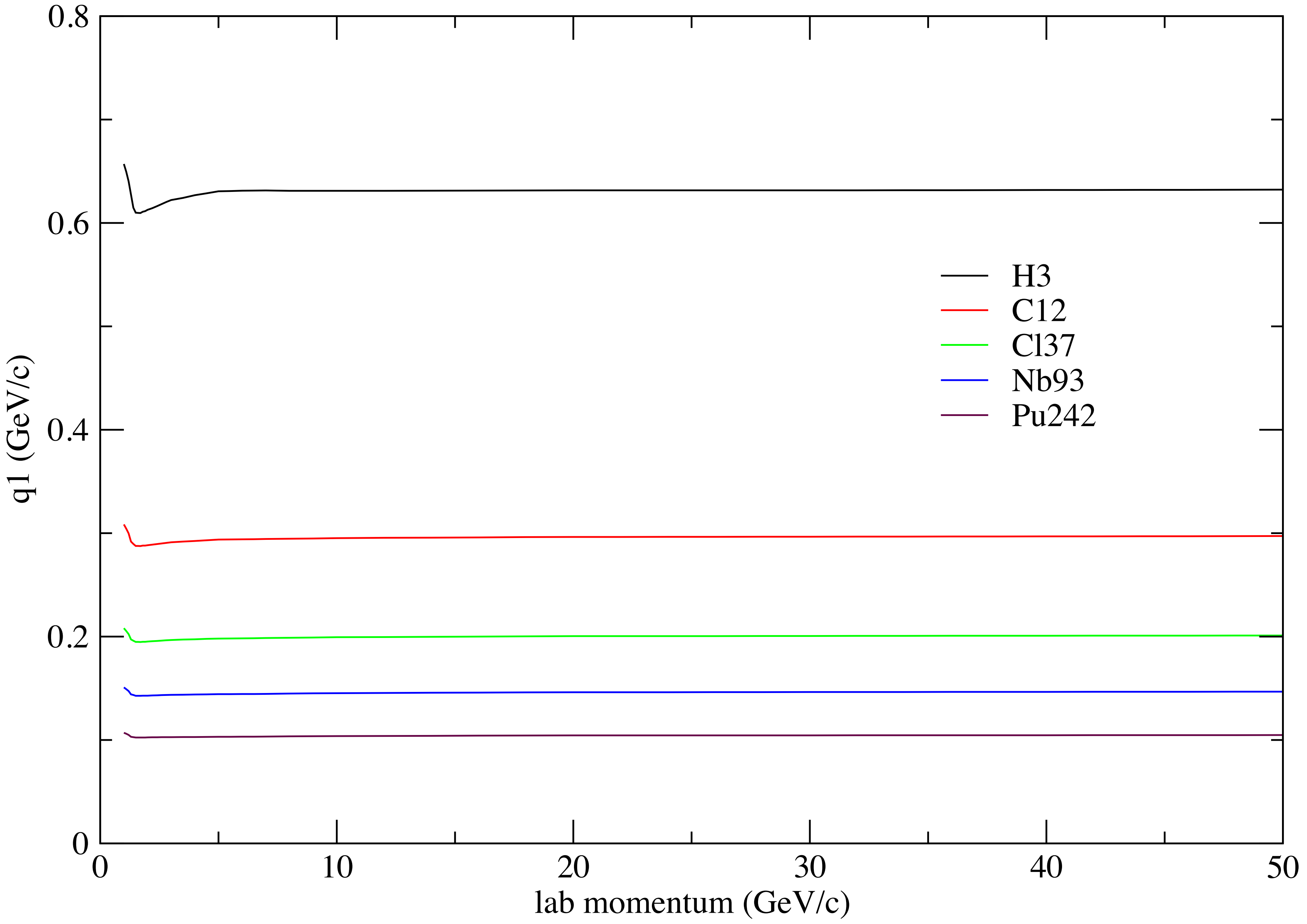

Figure 6

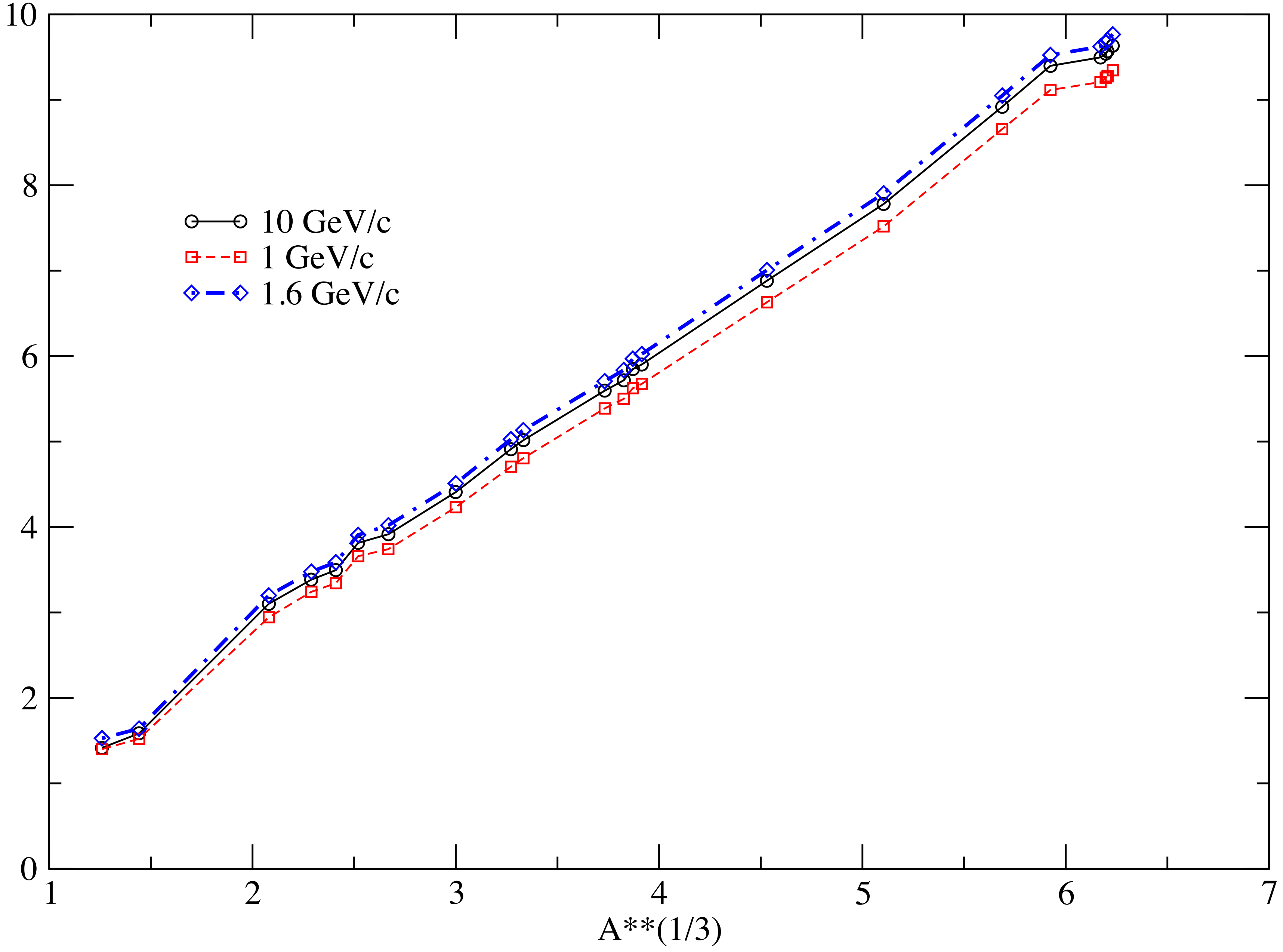
Variation of 1/q1 with mass number
10 GeV/c
1 GeV/c
1.6 GeV/c
1/q1 (c/GeV)
A**(1/3)
0
2
4
6
8
10
1
2
3
4
5
6
7

Monte Carlo Algorithm (3)

- Figure 7: sampling for the p + ^{12}C cross section from the data table at 2.2 GeV [3 GeV/c] and comparison with the original cross section calculation.
- Figure 8: sampling for p + ^{93}Nb at 4 GeV/c. Shown is the comparison of:
  - Original calculation;
  - Exact sampling from tabulation in library;
  - Sampling by interpolation between A = 60 and A = 133 and between p = 3 GeV/c and p = 5 GeV/c.

Figure 7

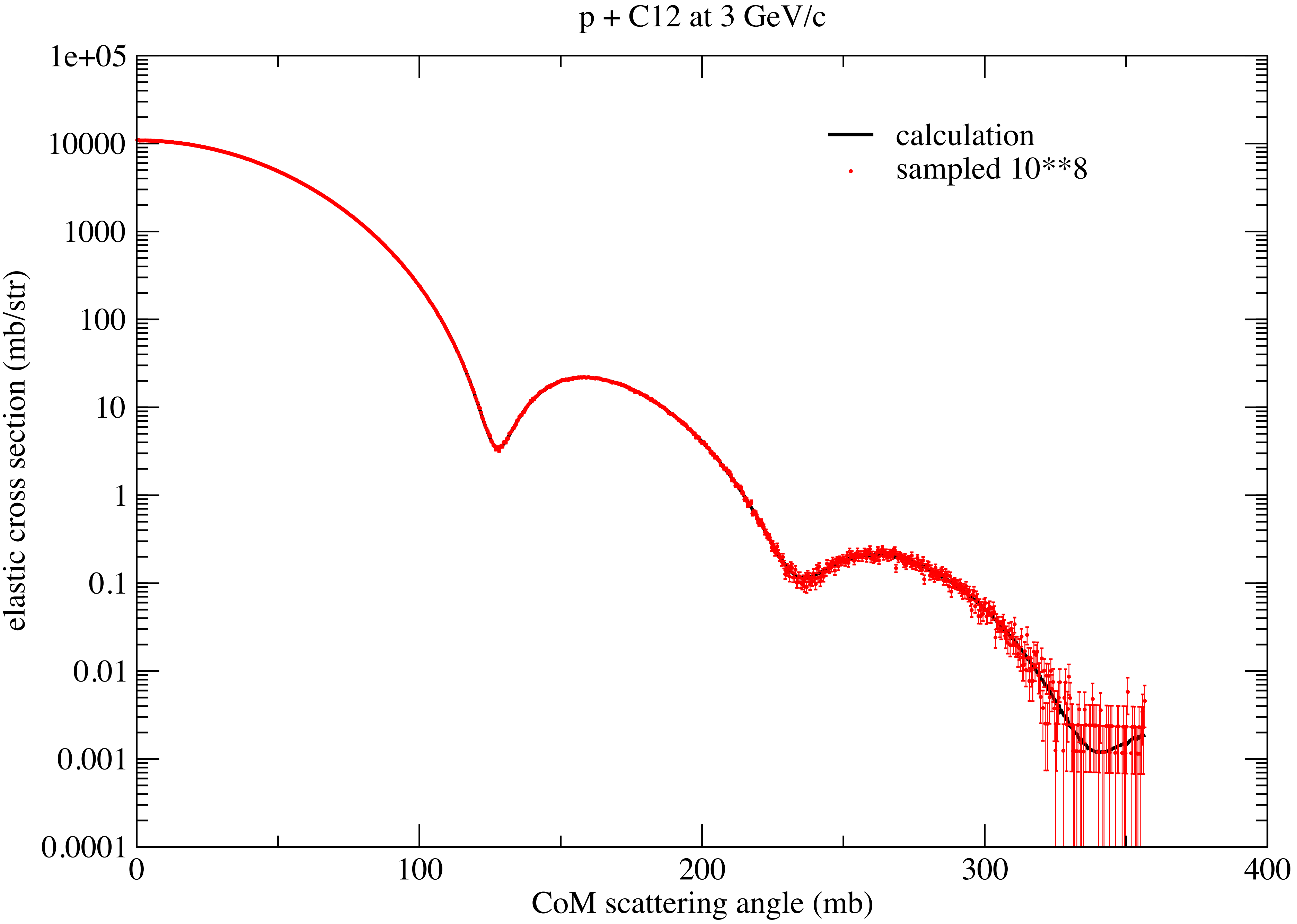
p + C12 at 3 GeV/c
elastic cross section (mb/str)
1e+05
10000
1000
100
10
1
0.1
0.01
0.001
0.0001
0
100
200
300
400
CoM scattering angle (mb)
calculation
sampled 10**8

Figure 8

p + Nb93 at 4.0 GeV/c

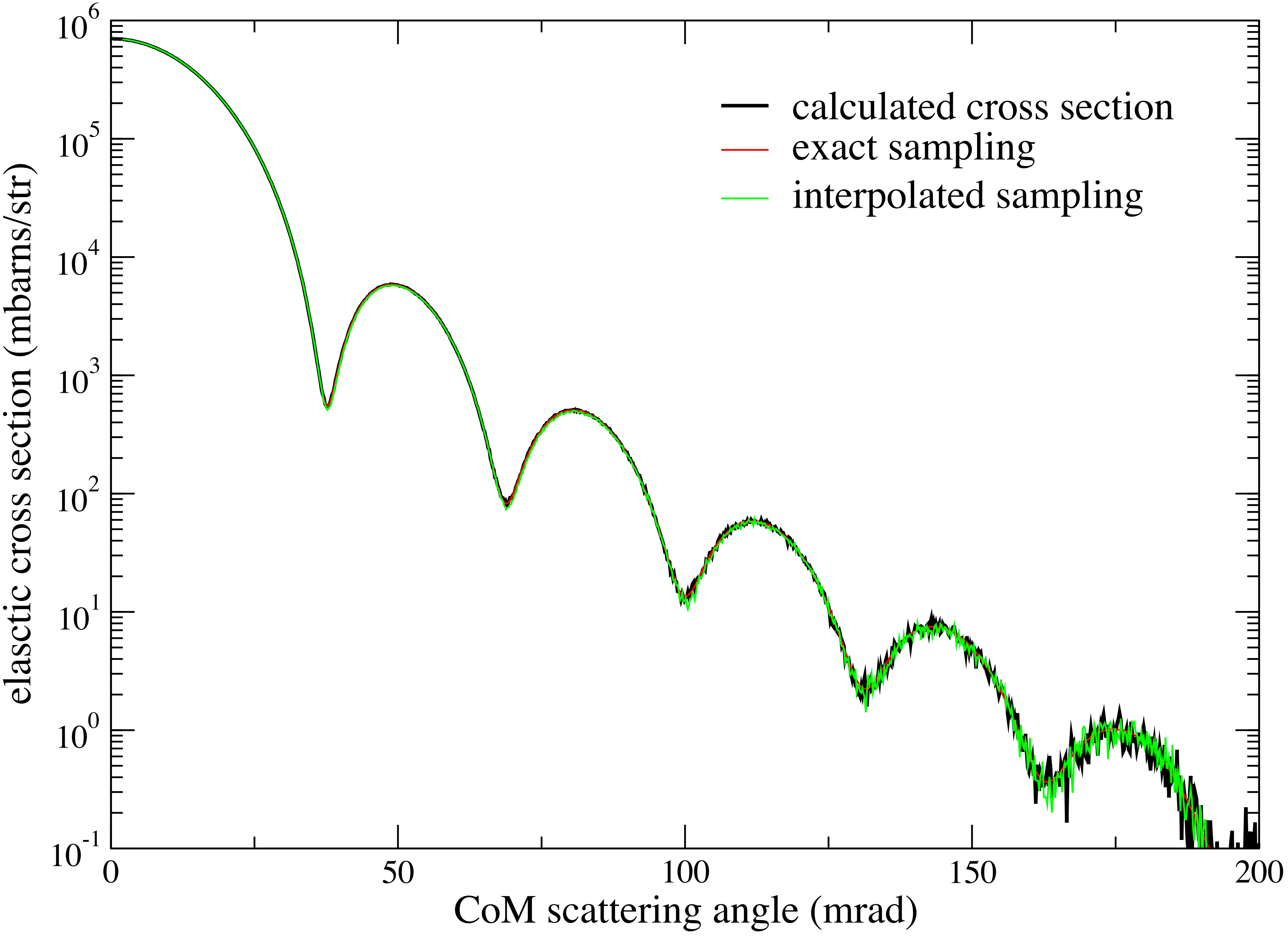

Validation (1)

- As part of the current effort, a compilation of comparisons with experimental proton scattering data is being prepared, including incident proton momenta from 1.75 GeV/c to 175 GeV/c.
- Examples of the comparisons are shown in figures 9, 10 and 11. In these figures, three components are shown with the total scattering distribution:

1. the multiple Coulomb scattering distribution of the uncollided beam;
2. the coherent nuclear elastic scattered component (this work), with multiple Coulomb scattering correction;
3. a simple model of incoherent (quasielastic) proton scattering[7].

Validation (2)

- Figure 9: Comparison of model calculations with the data of Schiz et al. at 70 GeV/c [8].
- Figure 10: Comparison of model calculations with the data of Bellettini et al. at 19.3 GeV/c. [9].
- Figure 11: Comparison of model calculations with the data of Blieden et al. at 10 GeV/c and 20 GeV/c [10].
- An attempt has been made to include the experimental angular resolution, as well as the incident beam angular and momentum spread, in the calculated results. Note that the experimental energy cuts eliminate most diffractive production from the data shown.

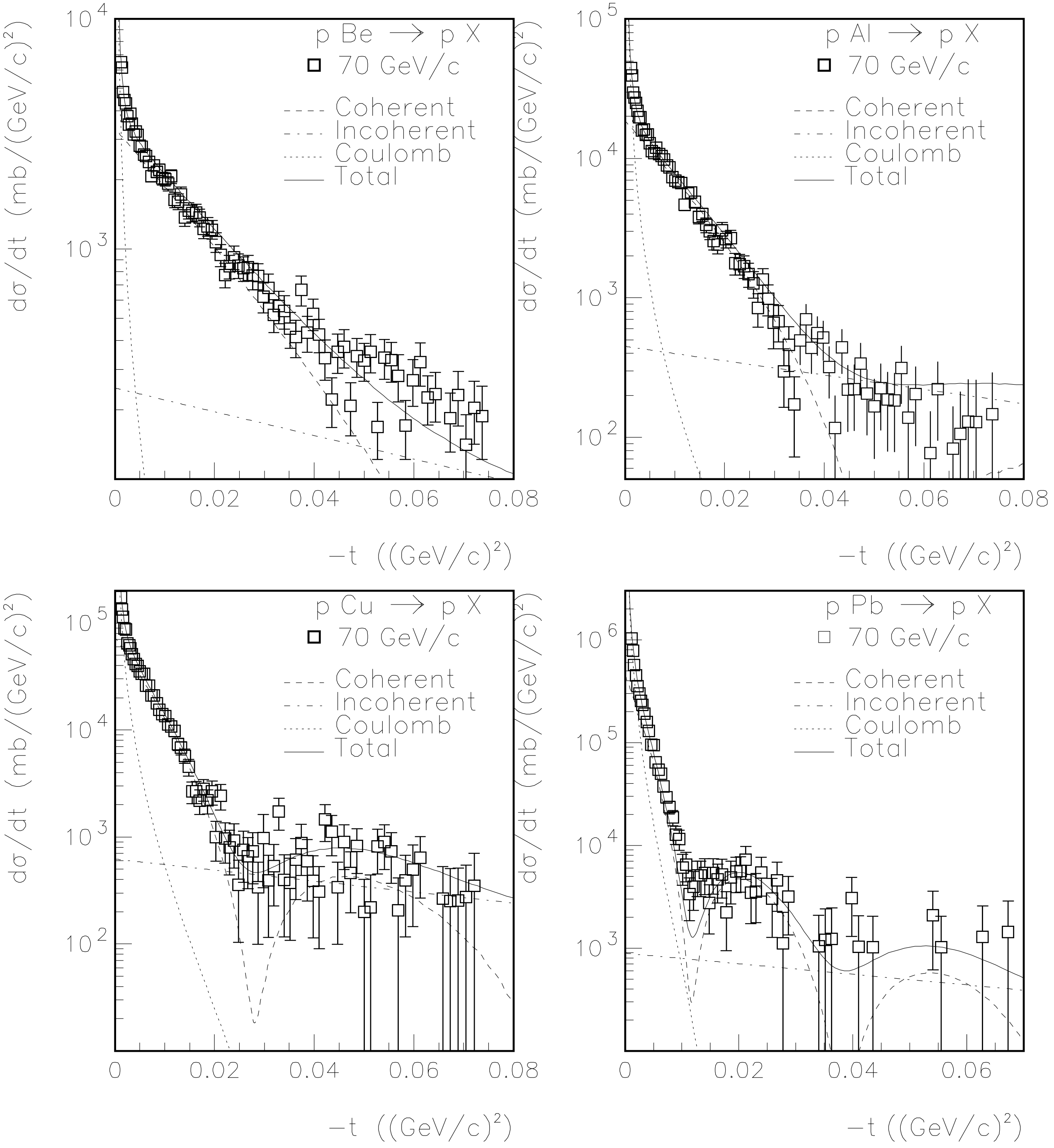
p Be → p X
70 GeV/c
Coherent
Incoherent
Coulomb
Total
p Al → p X
70 GeV/c
Coherent
Incoherent
Coulomb
Total
p Cu → p X
70 GeV/c
Coherent
Incoherent
Coulomb
Total
p Pb → p X
70 GeV/c
Coherent
Incoherent
Coulomb
Total
dσ/dt (mb/(GeV/c)²)
−t ((GeV/c)²)
10⁴
10³
10⁵
10²
10⁶
0
0.02
0.04
0.06
0.08

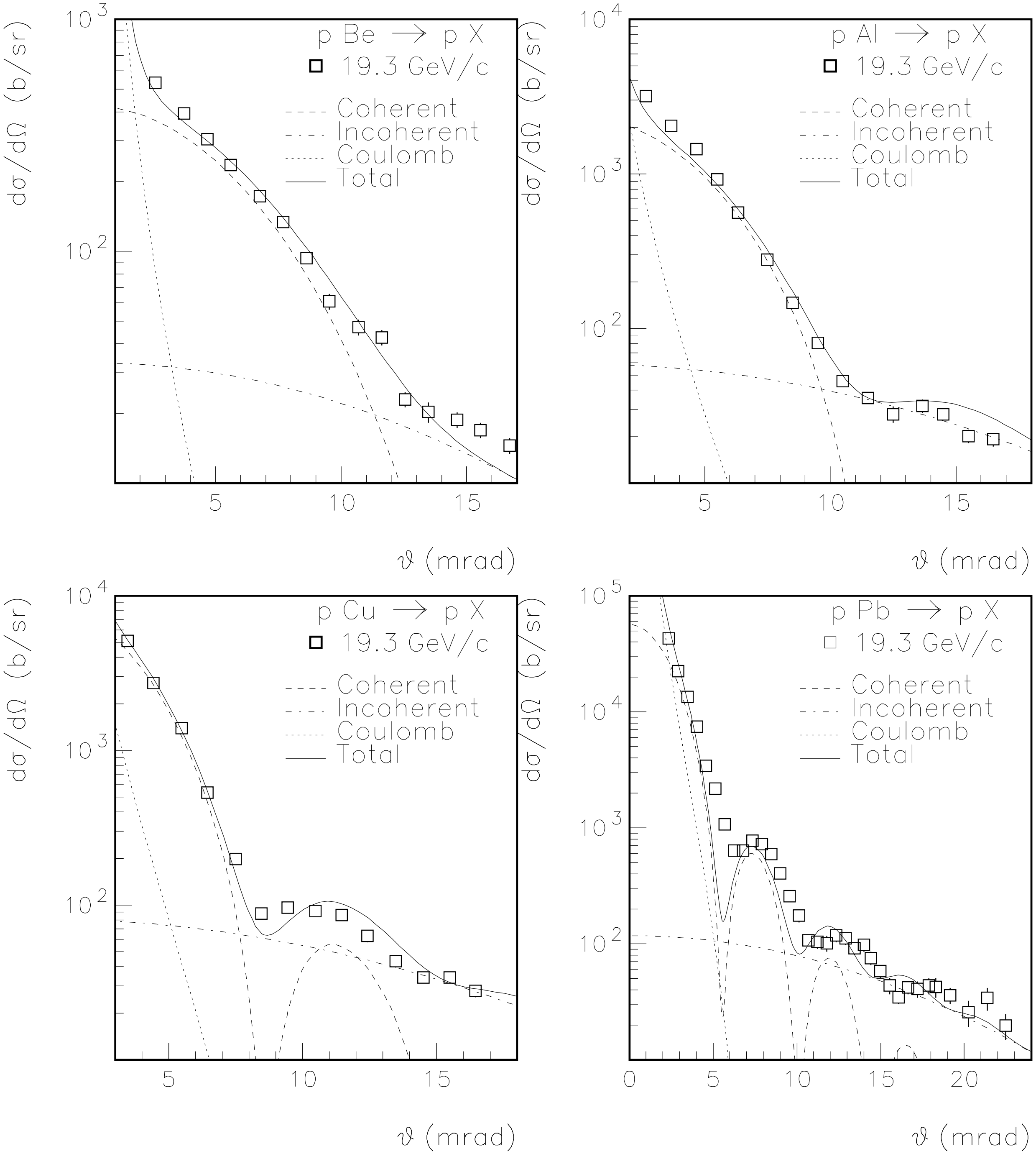

p Be → p X
19.3 GeV/c
Coherent
Incoherent
Coulomb
Total
dσ/dΩ (b/sr)
10^3
10^2
5
10
15
ϑ (mrad)
p Al → p X
19.3 GeV/c
Coherent
Incoherent
Coulomb
Total
dσ/dΩ (b/sr)
10^4
10^3
10^2
5
10
15
ϑ (mrad)
p Cu → p X
19.3 GeV/c
Coherent
Incoherent
Coulomb
Total
dσ/dΩ (b/sr)
10^4
10^3
10^2
5
10
15
ϑ (mrad)
p Pb → p X
19.3 GeV/c
Coherent
Incoherent
Coulomb
Total
dσ/dΩ (b/sr)
10^5
10^4
10^3
10^2
0
5
10
15
20
ϑ (mrad)

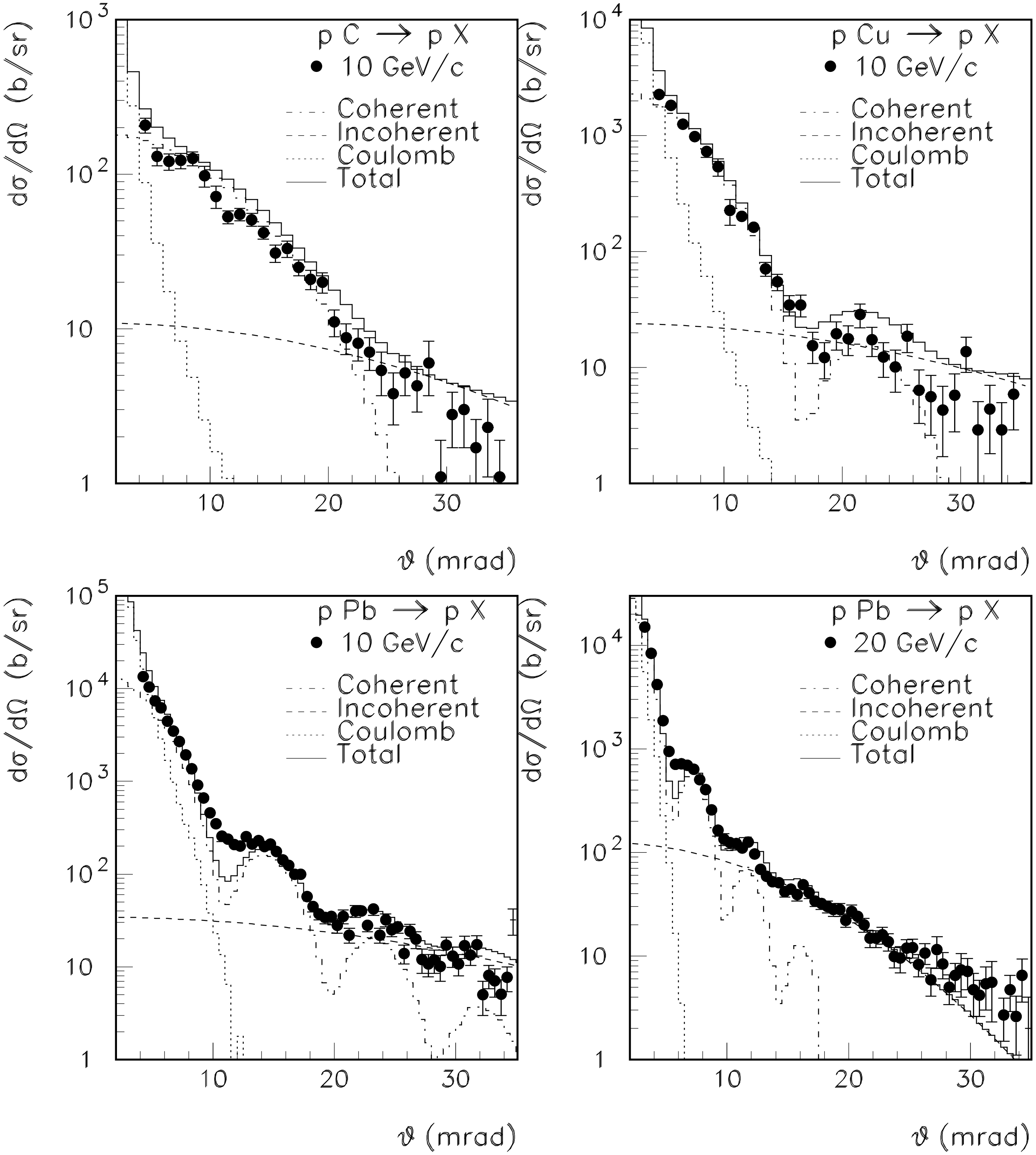
p C → p X
● 10 GeV/c
Coherent
Incoherent
Coulomb
Total
dσ/dΩ (b/sr)
10^3
10^2
10
1
10
20
30
ϑ (mrad)
p Cu → p X
● 10 GeV/c
Coherent
Incoherent
Coulomb
Total
dσ/dΩ (b/sr)
10^4
10^3
10^2
10
1
10
20
30
ϑ (mrad)
p Pb → p X
● 10 GeV/c
Coherent
Incoherent
Coulomb
Total
dσ/dΩ (b/sr)
10^5
10^4
10^3
10^2
10
1
10
20
30
ϑ (mrad)
p Pb → p X
● 20 GeV/c
Coherent
Incoherent
Coulomb
Total
dσ/dΩ (b/sr)
10^4
10^3
10^2
10
1
10
20
30
ϑ (mrad)

Validation (3)

- The multiple Coulomb scattering calculation is a new formulation[7] being developed for use in MCNP Version 5 in conjunction with the nuclear elastic scattering model.
- These comparisons show that using a Fermi nuclear form factor (rather than a Gaussian) is important for representing the multiple Coulomb scattering at momentum transfers near the minima for heavy nuclei.

Validation (4)

- In general, the nuclear elastic scattering representation described here provides a good overall description of the process.
- In many cases, the modeling does show deeper minima than the experimental data, even after corrections are applied.
- In the low energies examined, shifts in the location of the minima may perhaps be attributable to the neglect of nuclear-Coulomb interference in the model.

Conclusions (1)

- The Monte Carlo method described here achieves its objective of providing a highly accurate simulation of proton elastic scattering based on realistic optical model calculations.
- It is to be hoped that the present work will encourage the development of optical model calculations, including compilations for other incident particles.
- As additional calculated cross sections for low energies and for neutrons become available, the method will be provided as a general-purpose elastic scattering module; however, it remains to be determined that the representation is equally effective at lower energies.

Conclusions (2)

- The nuclear elastic scattering model and the new multiple Coulomb scattering model have been implemented and tested in MCNP5 (see figure 12); this enables radiographic simulation with an attenuated primary proton beam (no incoherent contribution.
- When modeling for the incoherent processes are incorporated in MCNP5 along with the nuclear elastic scattering model and the multiple Coulomb scattering model, validation with the experimental data will be possible.

Figure 12: 24 GeV/c Protons on 1 cm Tungsten

MCNP5 calulation: attenuated primary beam with no energy loss

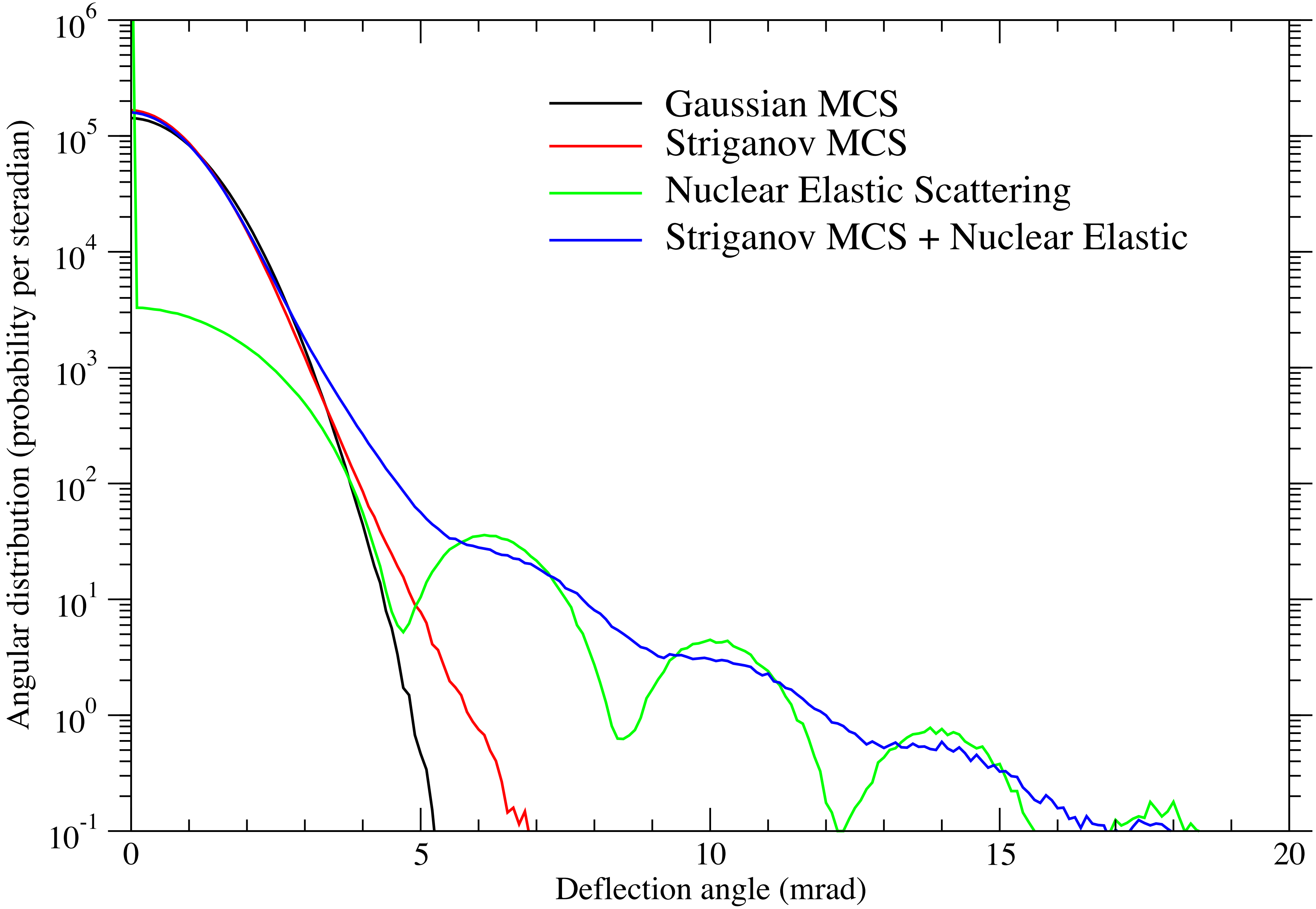

Conclusions (3)

- It will be validation with respect to experiments on macroscopic targets, where multiple Coulomb scattering obscures the details of the scattering process, that will set the priorities for improvements in the nuclear optical model.
- Development of multigroup cross sections based on the same calculations has been proposed. (R. C. Little, LANL X-5).
- Even though not correct in the details of the optical potential, the present model would provide a better representation of elastic scattering distributions for other hadrons than now available.

References

1. C. L. MORRIS, “Proton Radiography for an Advanced Hydrotest Facility,” Los Alamos National Laboratory Report LA-UR-00-5716, Los Alamos, 2000.
2. L. S. RODBERG and R. M. THALER, *Introduction to the Quantum Theory of Scattering*, Academic Press, New York, 1967.
3. L. C. LIU and C. M. SHAKIN, *Nuovo Cimento A* ***53***, 142 (1979).
4. K. GOULIANOS, *Phys. Rept.* ***3***, 169 (1983).
5. P. H. HANSEN and A. D. KRISCH, *Phys. Rev. D* ***15***, 3287 (1977).
6. R. J. GLAUBER and G. MATTHIAE, *Nucl. Phys.B* ***21***, 135 (1970).
7. S. STRIGANOV, personal communication.
8. A. SCHIZ et al., *Phys. Rev. D* ***21***, 3010 (1980).
9. G. BELLETTINI et al., *Nucl. Phys* ***79***, 609 (1966).
10. H. R. BLIEDEN et al., *Phys. Rev. D* ***11***, 14 (1975).

- *Contact: R E Prael (rep@lanl.gov)*